Parahydrogen discriminated PHIP at low magnetic fields

I. Prina, L. Buljubasich, R.H. Acosta *

FAMAF – Universidad Nacional de Córdoba, IFEG – CONICET, X5016LAE Córdoba, Argentina

A B S T R A C T

Parahydrogen induced polarization (PHIP) is a powerful hyperpolarization technique. However, as the signal created has an anti-phase characteristic, it is subject to signal cancellation when the experiment is carried out in inhomogeneous magnetic fields or in low fields that lack the necessary spectral resolution. The use of benchtop spectrometers and time domain (TD) analyzers has continuously grown in the last years and many applications are found in the food industry, for non-invasive compound detection or as a test bench for new contrast agents among others. In this type of NMR devices the combination of low and inhomogeneous magnetic fields renders the application of PHIP quite challenging. We have recently shown that the acquisition of J-spectra in high magnetic fields not only removes the anti-phase peak cancellation but also produces a separation of thermal from hyperpolarized signals, providing Parahydrogen Discriminated (PhD-PHIP) spectra. In this work we extend the use of PhD-PHIP to low and inhomogeneous fields. In this case the strong coupling found for the protons of the sample renders spin-echo spectra that have a great complexity, however, a central region in the spectrum with only hyperpolarized signal is clearly identified. This experimental approach is ideal for monitoring real time chemical reaction of pure PHIP signals.

1. Introduction

Hyperpolarization techniques have become relevant tools in the Nuclear Magnetic Resonance (NMR) community. In particular, Para-Hydrogen Induced Polarization (PHIP) is a relatively new technique which has significantly grown in the last two decades. Traditionally, NMR has dealt with the detection of nuclear spins in thermal equilibrium with an external magnetic field, resulting in a signal proportional to the small population difference, determined by a Boltzmann distribution, between the eigenstates of the Zeeman interaction Hamiltonian. One way to improve the NMR sensitivity consists in the direct hydrogenation of non-saturated compounds with molecular hydrogen enriched in its para-state (p-H_2) prior to the NMR experiment. In 1986, Bowers and Weitekamp reported a method to obtain large nuclear-spin polarization by exploiting the state of parahydrogen during a hydrogenation reaction [1]. The first results, where the reaction occurs in the presence of the same magnetic field of the NMR experiments, confirmed the predictions and inspired the acronym PASADENA (Parahydrogen And Synthesis Allow Dramatically Enhanced Nuclear Alignment) [2]. Since then, the technique has been continuously expanding in the field of NMR, as can be seen

by its wide range of applications, including the investigation of the kinetics of inorganic reactions in either homogeneously or heterogeneously catalyzed reactions [3–6], applications related with magnetic resonance imaging [7–10], intramolecular hyperpolarization transfer [11–15], or its use as a natural system with long lived states [16–21].

The NMR signal acquired after the reaction with p-H_2 in the PASADENA protocol is significantly different from the thermal counterpart. If we restrict the discussion to the case where the former parahydrogen protons form an isolated AX spin system in the target molecule, the spectrum displays two antiphase peaks [22,23]. This is due to the exclusive presence of a longitudinal two-spin order term in the density operator, which is present after the hydrogenation of the target molecule has been carried out. This is in turn the initial state for the NMR experiment, and is proportional to $I_1^z I_2^z$. Therefore, any source of field homogeneity results in partial signal cancellation, which can be quite considerable as the antiphase separation equals the J-coupling constant value, normally in the range of a few Hertz in most liquid samples. The most common situation, when working at high magnetic fields, is that the p-H_2 protons are weakly coupled to other protons in the product molecule, that is, the chemical shift difference δv is much higher than the J-coupling constant. In this case the spectrum consists of a collection of antiphase signals centered at the chemical shifts of the corresponding [1]H's. The inverse situation is present,

* Corresponding author.
  E-mail address: racosta@famaf.unc.edu.ar (R.H. Acosta).

for instance, when working at low magnetic fields, in which the system is in the inverse weak coupling regime ($\delta v \ll J$). Even in this case chemical shift and J-coupling information can be acquired with PHIP, and experiments in a home-made system with a magnetic field lower than 20 mT and homogeneity below one ppm have been recently reported [24–26].

An intermediate regime is present when using commercial benchtop spectrometers, or time-domain (TD) analyzers. At these low magnetic fields, typically ranging from 0.5 to 1.4 Tesla, strong coupling will most certainly be present ($\delta v \sim J$). Additionally the general low homogeneity of these magnetic fields will produce a significant cancellation in PASADENA experiments. The use of spin echoes was recently introduced in a way to refocus the magnetic field inhomogeneities, in order to obtain PHIP signals in a TD analyzer operating at 0.54 Tesla, namely time domain PHIP (TD-PHIP) [27]. In this case the echo time would be given by $1/(4J)$ for a two-spin system in the weak coupling regime. However, in larger spin systems the echo time must be chosen to maximize the signal based on the distribution of J-coupling values of the system [10]. At low field extreme care must be taken before applying the same strategy, as the top of the spin echoes are no longer free of chemical shift evolution. These results are of great importance for an area that is increasingly growing within the applications of TD-NMR and even in high resolution low-field spectroscopy [28,29]. The use of hyperpolarization as a contrast agent or site specific tracer could be very important in terms of a simplification of the information obtained on the particular systems under study.

We have recently addressed the problem of inhomogeneous broadened multiplets in PASADENA experiments at high magnetic field by acquiring J-spectra under PHIP conditions. In the weak coupling approximation the evolution with the terms in the spin Hamiltonian linear on spin operators, as magnetic field inhomogeneities or chemical shifts, are refocused during a CPMG-like train of radio-frequency (rf) pulses [30,31], whereas evolutions with the terms in the spin Hamiltonian bi-linear on spin operators, e.g. the J-coupling evolution, remain unmodified [32]. In principle very complex spectra are expected in this type of experiment as all the chemical shift information is lost, thus all the multiplets collapse at zero frequency. The information can be simplified by performing data acquisition with a digital filter accurately centred at the desired multiplet, namely partial J-spectroscopy. We were able to obtain partial J-spectra practically free of peak cancellation [33]. Additionally, the pulse train can be used to separate contributions between parahydrogen induced signals and those arising from thermal backgrounds. These can be originated by a larger amount of molecules with resonance frequencies near the frequencies of the sites in the target molecule occupied by the former p-H_2 protons (e.g. solvent signals) or by thermal contributions of the product molecule when a reaction advances and the conversion is lower [34]. The difference in the evolution of polarization terms compared to longitudinal two-spin order terms under the pulse train provides a mechanism to obtain Parahydrogen-Discriminated PHIP (PhD-PHIP) signals [35] which appear shifted by half of the spectral width compared to thermal signals.

In the present work we explore the performance of the method at lower magnetic fields, where the weak coupling approximation is no longer valid. We demonstrate that PhD-PHIP can be applied at low and inhomogeneous magnetic fields in a TD-analyzer; in this case all the spins are strongly coupled and a digital filter can no longer be implemented to remove the presence of large background signals or the superposition of different multiplets at zero frequency. We present numerical simulations for two and three spin systems showing that signal discrimination occurs even in the strong coupling regime. Experimental results in a complex spin system are included along with an example where the dynamics of a chemical reaction of only the hyperpolarized fraction of the sample is monitored.

2. Theory

2.1. Evolutions under weak and strong couplings

In an isotropic liquid, the rapid tumbling of molecules averages out the direct dipole–dipole coupling between nuclear spins. The interaction of N spins-1/2 is, therefore, fully described by the isotropic part of the chemical shift and the isotropic J-coupling (or indirect dipole–dipole coupling) Hamiltonians [22,23].

In the presence of a sufficiently high magnetic field B_0, all the spins are weakly coupled, i.e. the chemical shift difference between any pair of spins is much larger than their J-coupling constant. The Hamiltonian in the rotating frame can be written as [22,23]:

$$\mathcal{H}_{\text{weak}} = \sum_{i=1}^{N} 2\pi v_i I_i^z + \sum_{i<j}^{N} 2\pi J_{ij} I_i^z I_j^z. \tag{1}$$

As the chemical shift and J-coupling terms in Eq. (1) commute, the spin evolution can be calculated by taking into account one term at a time. During a CPMG pulse sequence, the evolution with the terms of the Hamiltonian linear on spin operators, as the first term in Eq. (1) are refocused at $t = n t_E$, with t_E being the echo time. On the other hand, evolutions with the terms in the Hamiltonian bilinear on spin operators, as the second term in Eq. (1), are unaffected by the rf pulses. The stroboscopic acquisition of the NMR signal at $t = n t_E$ and the subsequent Fourier transformation yield what is known as J-spectrum [36,37], a superposition of multiplets centered at zero frequency, with no chemical shift information. By setting a digital filter centred at the desired chemical shift frequency during the acquisition, all the other multiplets can be filtered out and a partial J-spectrum is obtained [37].

In the context of weak coupling limit, we have recently demonstrated that the PHIP density operator just after the chemical reaction in PASADENA, which is essentially a linear combination of longitudinal two-spin order terms $\left(\propto I_i^z I_j^z \right)$, evolves appreciably differently during the train of refocusing pulses compared to the thermal density operators (i.e. polarization terms). PHIP-induced signals present and odd–even modulation with the 180° pulses (resembling the evolution of thermal signals under a Carr–Purcell pulse sequence). The result of the application of a Fast Fourier Transform (FFT) to such a data set is the combination of two different spectra centered at half of the spectral width with respect to each other. Thus, a natural mechanism for signal separation is present [35], allowing the discrimination between signals originating from parahydrogen from that originated from thermal backgrounds, which could mask out the hyperpolarized contributions.

In low magnetic fields the situation is manifestly different. The spins are no longer weakly coupled and the full isotropic part of the J-coupling Hamiltonian is retained, leading to:

$$\mathcal{H}_{\text{strong}} = \sum_{i=1}^{N} 2\pi v_i I_i^z + \sum_{i<j}^{N} 2\pi J_{ij} \mathbf{I}_i \cdot \mathbf{I}_j. \tag{2}$$

The chemical shift and J-coupling Hamiltonians in Eq. (2) do not commute and the evolution must be calculated with the full $\mathcal{H}_{\text{strong}}$. Consequently, chemical shift information is also present at the top of the spin echoes, introducing additional modulations to the spin echo amplitudes which are strongly dependent on t_E. Freeman and Hill [37] refer to this kind of spectra as *spin-echo spectra*. At the end of the chemical reaction, the density operator contains not only two-spin order terms, as polarization difference and zero-quantum terms might be present depending on the chemical shifts and the J-coupling network. In order to determine a priori if there will be a separation between PHIP and thermal contributions in *spin-echo spectroscopy* numerical simulations are then mandatory.

2.2. Simulations of the evolution under strong couplings for 2- and 3-spin systems

As stated above, the full Hamiltonian $\mathcal{H}_{strong}$ has to be considered in the evolution of density operators during a CPMG-like pulse sequence. To explore the feasibility of achieving a frequency discrimination of PHIP from thermal signals we have performed numerical simulations on 2- and 3-strongly coupled spin systems using a 45° rf pulse for excitation and an MLEV-4 phase cycle for the train of refocusing pulses [38]. The dynamics during the pulse sequence were calculated by solving the Liouville–Von Neumann equation at $t = nt_E$ with the Hamiltonian of Eq. (2). A FFT of the simulated data set was then carried out without the usual shift of the spectrum by $N/2$, being N the number of points in the spectral dimension [35], rendering simulated spin-echo spectra.

As usual, the thermal initial density operator before the first r.f. pulse corresponds to the total polarization operator, $\rho^{th}(0) \propto \sum_i I_i^z$. In the case of PHIP, the chemical reactions have to be considered. A single reaction consists in the evolution of the p-H$_2$ density operator with the Hamiltonian of the product molecule until $d\rho^{pr}/dt = 0$. The ensemble average is obtained by taking the time average of a single evolution of ρ^{pr} assuming that the chemical reaction lasts longer than the characteristic time of any internal evolution. This yields the PHIP density operator at the end of the reaction $\rho^{PH}(0)$ (further details of the simulation method can be found in Refs. [15,39]).

First we consider the case where the former parahydrogen protons (H$_1$ and H$_2$) form an isolated strongly coupled two-spin system at the product molecule, i.e. an AB spin system [23]. Simulations were carried out with the following conditions: $v_1 = 1$ ppm, $v_2 = 1.5$ ppm, $J_{12} = 7$ Hz, $B_0 = 0.45$ Tesla (corresponding to $\omega_0/2\pi = 19.86$ MHz proton Larmor frequency) and $t_E = 15$ ms. The density operator after the chemical reaction results in:

$$\rho_{AB}^{PH}(0) = -1 \times I_1^z I_2^z + 0.4772 \times (I_1^z - I_2^z) \\ - 0.3183 \times (I_1^x I_2^x + I_1^y I_2^y) + 0.0125 \times (I_1^x I_2^y + I_1^y I_2^x), \qquad (3)$$

and the simulated spin-echo spectrum (see Fig. 1A) presents a single antiphase doublet, which is the fingerprint of longitudinal two-spin order, at the center of the spectral window. If the system is consists in equal parts of PHIP and thermally polarized species, the initial density operator is then: $\rho_{AB}^{PH}(0) + \rho_{AB}^{th}(0)$. In this case the spin-echo spectrum shown in Fig. 1B has the additional in-phase doublet at the border of the spectral window corresponding to the thermal signals.

The next step in complexity is to consider the case where the former parahydrogen protons are strongly coupled to each other as well as to a third spin in the target molecule, forming a strongly coupled three-spin system (or ABC spin system [23], as schematically shown in Fig. 1C). The values used in this simulation are: $v_1 = 6.0$ ppm, $v_2 = 5.8$ ppm, $v_3 = 6.25$ ppm, $J_{12} = 10.2$ Hz, $J_{13} = 17.2$ Hz, $J_{23} = 1.8$ Hz, $B_0 = 0.45$ Tesla and $t_E = 15$ ms. The density operator after the chemical reaction is composed by a series of terms, and can be written in a compressed manner as:

$$\rho_{ABC}^{PH}(0) = \sum_{(i<j)=1}^{3} \alpha_{ij} I_i^z I_j^z + \sum_{(i<j)=1}^{3} \lambda_{ij} \left(I_i^x I_j^x + I_i^y I_j^y \right) + \sum_{i=1}^{3} \beta_i I_i^z \\ + \delta \left(I_1^z I_2^x I_3^x + I_1^z I_2^y I_3^y \right) + \epsilon \left(I_1^x I_2^z I_3^x + I_1^y I_2^z I_3^y \right), \qquad (4)$$

where $\alpha_{ij}, \beta_i, \lambda_{ij}, \delta$ and ϵ are constants obtained from the simulation. The spin-echo spectrum in this case presents an antiphase doublet in the center of the spectral window plus contributions from higher spin order terms that fall in the border of the spectral width, as shown in Fig. 1C. These contributions cannot be separated from the ones arising from thermally induced signals as shown in Fig. 1D, where the same fraction of PHIP and thermal density operators were used as the initial state of the system.

This is the major difference with the weak coupling limit, in which all the information of the hyperpolarized species is in the center of the spectrum, and thus separated from thermal signals. It is to be expected that larger spin systems will have a much more complex structure than the simple case addresses in our simulation, however it is quite clear that a significant fraction of the hyperpolarized signals will be located in the center of the spectral window, and more important, that only hyperpolarized signals will be in this spectral region, thus PhD-PHIP can still be applied at low field and has a great potentiality to monitor hydrogenation processes as discussed in the last section.

3. Results and discussion

3.1. Thermal and PHIP spin-echo spectra

In order to test the behavior of PhD-PHIP at low magnetic fields, experiments were performed in a Bruker Minispec mq20 operating at $\sim$20 MHz ^{1}H-Larmor frequency ($B_0 \sim 0.45$ Tesla). The B_0 inhomogeneity results in a line width of $\sim$200 Hz for the used sample volume. The hyperpolarized molecules were obtained by means of the chemical reaction depicted in Fig. 2A, consisting in the hydrogenation of 1-hexyne into 1-hexene. This complex spin system is suitable to evaluate the performance of the method. The former parahydrogen protons, labelled as H$_1^*$ and H$_2^*$, occupy chemically inequivalent sites at the product molecule, interacting with three other spins with relatively large coupling constants. Additionally, all the protons are separated $\lesssim$5 ppm, which represents a range of 100 Hz at the magnetic field strength of the spectrometer.

As the chemical shift differences relative to the coupling constants for the protons H$_1^*$, H$_2^*$, H$_3$ and H$_{4-5}$ are:

- $\left| v_1^* - v_2^* \right|/J_{12} \sim 1.7$
- $\left| v_1^* - v_3 \right|/J_{13} \sim 1.0$
- $\left| v_2^* - v_3 \right|/J_{23} \sim 0.36$
- $\left| v_1^* - v_4 \right|/J_{14(5)} \sim 10.5$
- $\left| v_2^* - v_4 \right|/J_{24(5)} \sim 48$ we assume that negligible hyperpolarization will be transferred to H$_{4-5}$. Therefore, nine protons with thermal polarization remain in the product molecule and ten from the 1-hexyne molecules which have not yet been hydrogenated. The signals corresponding to these protons will interfere with the PHIP signal.

Fig. 2B shows the spin-echo spectra before the hydrogenation process acquired with $t_E = 15$ ms. A small signal in the center of the spectral window is present due to imperfections in the 180° pulses which are not present if a 90° excitation pulse is used. The thermal signal is located at the border of the spectrum as predicted. After the chemical reaction with p-H$_2$, a dominant antiphase doublet appear at the center of the spectral window (Fig. 2B), which are much stronger than those in the borders. It is worth noting that both spectra are displayed in the same vertical scale, and that many features appear in the baseline of the hyperpolarized spectra, which greatly exceed the noise level. We have carried out numerical simulations on a seven spin system (data not shown) and, even though the exact features cannot be reproduced with such a small system, the presence of the structure indicates that these signals arise from higher spin order terms. The relative intensity of the antiphase peaks with respect to the in-phase ones that appear on the spectrum borders is dependent on the echo time used, as we are dealing with a strongly coupled system.
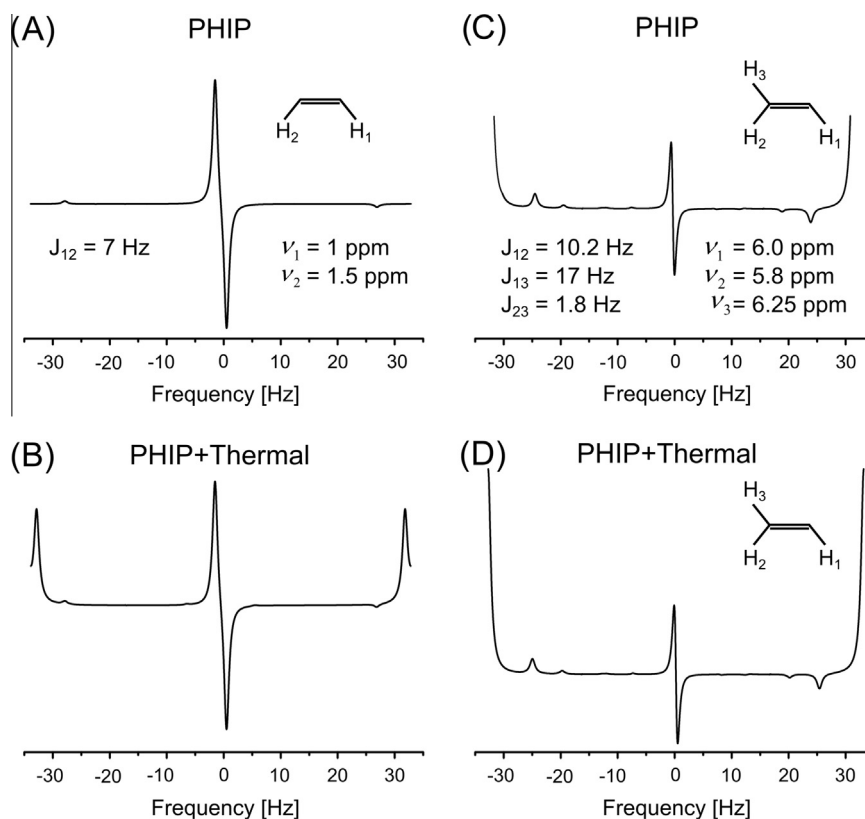
Fig. 1. (A) Simulations of a spin-echo spectrum using 2 strongly coupled spins in a low magnetic field. (B) Same as (A) but adding a thermal operator to the PHIP initial density operator. (C) Simulated spin-echo spectra of 3 strongly coupled spins without and with (D) thermal operators in ρ_0^{AMB} respectively.
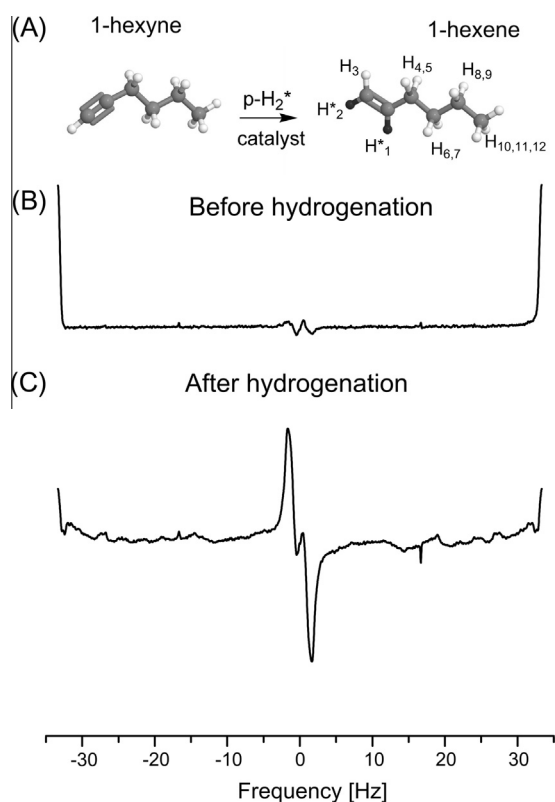
Fig. 2. (A) Scheme of the chemical reaction from 1-hexyne (educt) to 1-hexene (product). ^{1}H spin-echo spectra of 1-hexyne (B) and hyperpolarized 1-hexene (C) for $t_E = 15$ ms.

We now turn our attention to the effect of the echo time on the spin-echo spectra. Each spectrum in the left column of Fig. 3 corresponds to an independent experiment of enriched p-H$_2$. On the right column the spectra of a commercial sample of the product molecule are shown. All the spectra were normalized to the highest feature of the corresponding sample spectrum obtained for $t_E = 21$ ms. For the product molecule, the area of the spectra slightly increases with decreasing echo time, consistent with the fact that for shorter echo times the first digitalized echo point has a higher intensity. However, for $t_E = 3$ ms a loss of intensity indicates that the sequence timing is no longer optimized for this sample. In the case of the hyperpolarized sample, for short echo times ($t_E = 3$ ms) the antiphase doublet at zero frequency is of the same order of magnitude as that of the thermal species (right column). These small antiphase signals are a consequence of small errors in the rf pulses, as confirmed by numerical simulations. For longer echo times ($t_E = 9$ ms) the hyperpolarized signal exceeds the level of the artifact present in the center of the spectral window and a destructive interference due to high order terms in the density operator of the hyperpolarized species renders a small signal in the borders of the spectral window. For longer echo times ($t_E = 15$ ms) the hyperpolarized signal maintains its amplitude but is better resolved. Again, thermal signals are cancelled out at the borders of the spectrum. As already mentioned, many features that exceed the noise level appear for these echo times. For even longer pulse separations ($t_E = 21$ ms) these features increase with respect to the central antiphase signal. It must be taken into account that, as no digital filtering is included in this type of experiment, the presence of aliasing cannot be disregarded at longer echo times. A precise description of the features of these spectra require numerical simulations considering the full twelve spin-system, which is currently too demanding for standard calculations. Even
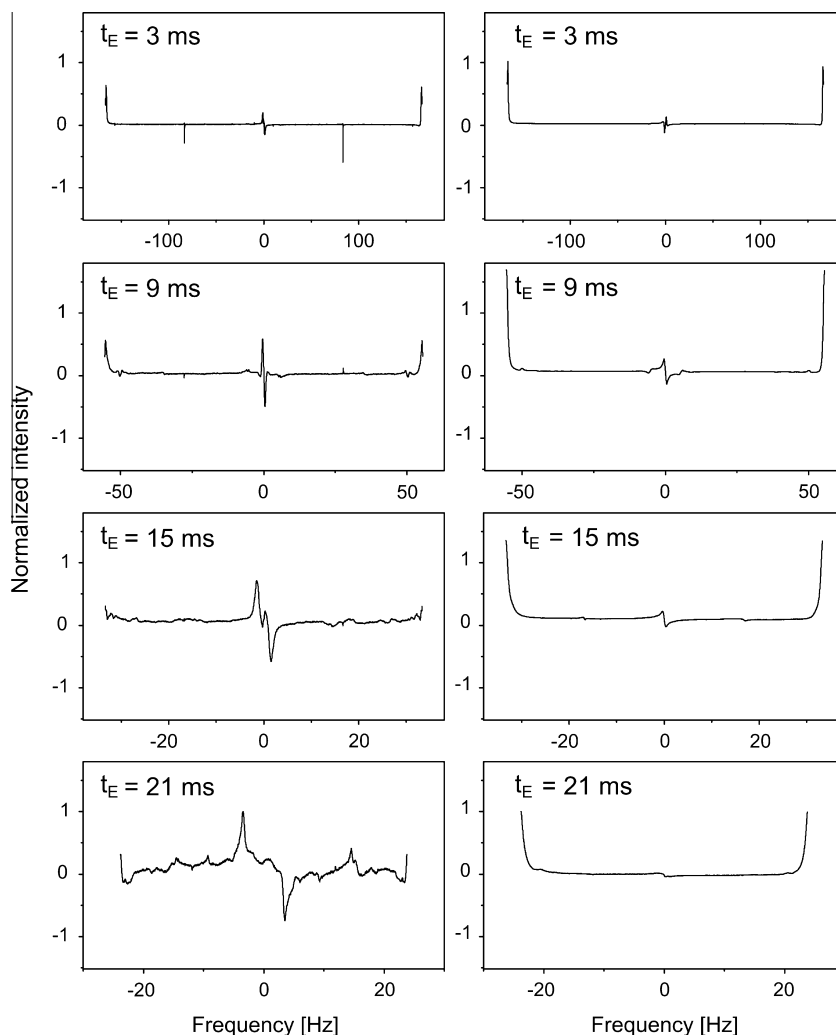
Fig. 3. Spin echo spectra for different echo times. For short t_E the evolution with J-couplings is perturbed by the rf pulses. Left: [1]H spin-echo spectra of hyperpolarized 1-hexene and thermal 1-hexyne. Right: [1]H spin-echo spectra of 1-hexene diluted and deuterated acetone.

though the spectra are far too complex to be completely described, the presence of the antiphase signal in the center of the spectrum is a clear indicator of the presence of hyperpolarization and can be used for on-line chemical reaction monitoring, free of thermal signal contributions. A correct choice of the echo time depends on the particular system under study, and can be determined by comparing the result obtained on the product molecule as shown before.

3.2. Monitoring a reaction at low magnetic field

For this particular system and magnetic field intensity, $t_E = 15$ ms seems to be a reasonably choice to observe the PHIP signal by means of the PhD-PHIP method. A non-reacted sample was placed in the bore of the magnet and left for 15 min. in order to reach thermal equilibrium. In order to obtain a hyperpolarized signal, bubbling of p-H_2 inside the NMR tube was performed during 20 s. A 5 s waiting time is left before the pulse sequence application to ensure that the sample is free of gas bubbles. Results are displayed in Fig. 4, where the time variable t_r denotes the time elapsed since the reaction has started. The intensities were obtained by integration in the range as shown in the figure inset.
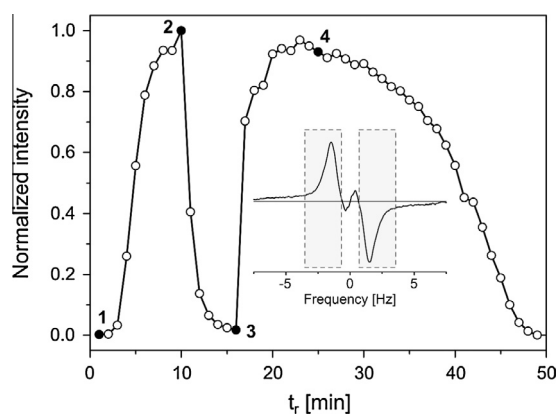
Fig. 4. Reaction of 1-hexyne monitored with the PhD-PHIP protocol. As the reaction time increases the amount of thermal species increases accordingly, however, if pH$_2$ is not provided to the sample (point 2), the signal level decreases to zero intensity (point 3), reflecting the fact that in the central part of the spectral window only hyperpolarization is detected. The point 4 is included to point out that the signal intensity is lower than the maximum achieved intensity, due to the fraction of the educt molecules that have reacted and will be thermally polarized for the rest of the experiment.

The higher frequency peak area was inverted in order to render non-zero values.

The point labelled as **1** is the initial state, prior to the first bubbling. The subsequent data has negligible intensity as the catalyst is to be activated before a pairwise hydrogenation with the target molecule can occur. This is an indicator of the accuracy of the integration range selection. After two bubbling/measurement cycles non-negligible signal is obtained, and the intensity grows rapidly until the point marked as **2**, corresponding to ten cycles. Bubbling was interrupted while measurements were performed at the same time intervals, to show that the intensities recorded are related only to PHIP. Five spin-echo spectra were collected with decreasing intensity, which are present due to ongoing reaction between target molecules and dissolved gas remaining from previous bubbling steps. Finally, all the residual gas was consumed and the state where the sample has only thermally polarized spins is reached (point **3**).

As the bubbling/measurement cycles are continued, a revival of the reaction occurs and the intensities reach almost the same level as before. At point denoted as **4** the intensity represents $\sim 90\%$ of the maximum achieved intensity, as part of the 1-hexyne has reacted into the product molecule between points **2** and **3**. After 50 min since the start of the experiment, the reaction has ceased. Consequently, the central part of the spin-echo spectrum has zero intensity. It must be taken into account that a substantial degree of evaporation of the sample occurred in the final stages of the experiment, which must also be considered to interpret the rapid decay present after 35 min.

This simple experiment shows that PhD-PHIP is an extremely sensitive tool to monitor chemical reactions at low magnetic fields even with a poor degree of homogeneity.

4. Experimental details

4.1. NMR experiments

Experiments were carried out at 0.45 Tesla with a Bruker Minispec mq20 spectrometer. A modified CPMG pulse sequence was used, where the initial 90° pulse was replaced by a 45° and a pair-alternated phases, transverse to the excitation pulse, were adopted for the refocusing pulses ($yy\overline{yy}$). The pulse lengths were set to 1.4 µs and 5.2 µs for exciting and refocusing pulses respectively. The temperature of the sample was controlled during the experiments using a Bruker BVT3000 temperature control. A variable number of refocusing pulses were used depending on t_E in order to acquire the signal time decay, additionally, all the experiments were acquired in a single shot. Hyperpolarization was achieved by bubbling p-H_2 into the sample settled within the coil for 20 s. In all cases a waiting period of 5 s was introduced before detection to ensure that no bubbles were present in the sensitive volume.

4.2. Sample preparation

Samples were prepared under controlled nitrogen atmosphere. They consisted in a solution of 0.443 g of acetone-d_6, 0.015 g of 1-hexyne and 0.010 g of catalyst (Rhodium complex: CAS 79255-71-3; $[Rh(dppb)(COD)]BF4$). All components were acquired from Sigma Aldrich and used without further purification.

Parahydrogen was prepared by letting normal hydrogen to repose at 77 K in activated charcoal during 30 min., being afterward stored in stainless steel cylinders (Swagelok, Germany) at ~ 4 bars. Plastic 4 mm OD tubing was used for the transfer lines and electromagnetic valves (Festo KG, Esslingen, Germany) were used to accurately control the gas delivery to the sample.

5. Conclusions

In this work we show that PhD-PHIP can be applied even in the limit of strong coupling, i.e. when the chemical shift difference between the former parahydrogen protons in the target molecule is comparable to their coupling constant. In this condition spin-echo spectra are obtained, in contra-position with the *J*-spectra obtained in the weak coupling limit. In both cases discrimination of PHIP signals from thermal ones is achieved by acquiring the evolution of the signal in the top of a CPMG-like sequence. Even though the separation is not complete in the strong coupling regime, the most significant part of the PHIP signals present an odd–even effect that render the spectral separation upon a fast Fourier transformation. We showed that the method is extremely sensitive and can be applied for instance to monitor online chemical reactions.

The possibility to detect the degree of hyperpolarization achievable with a low-cost portable magnet is very promising and will most certainly widen the applications of PHIP. The gas delivery setup is quite simple, as in these types of magnets there is practically no stray field as is the case in high field magnets. Additionally, the sequence is very robust and of straightforward application even for non NMR experts. Nevertheless, extension of this approach to even lower magnetic fields is still an open subject. The signals in the spin-echo spectrum center arise only from PHIP independently of the magnetic field intensity. However, the fraction of hyperpolarization after the chemical reaction remains in a combination of singlet states, with the consequent signal reduction.

References

[1] C.R. Bowers, D.P. Weitekamp, Phys. Rev. Lett. 57 (1986) 2645–2648.
[2] C. Bowers, D. Weitekamp, JACS 109 (1987) 5541–5542.
[3] J. Natterer, O. Schedletzky, J. Barkemeyer, J. Bargon, S. Glaser, J. Magn. Reson. 133 (1998) 92–97.
[4] S.B. Duckett, D. Blazina, Eur. J. Inorg. Chem. 2003 (2003) 2901–2912.
[5] S.B. Duckett, C.J. Sleigh, Prog. Nucl. Magn. Reson. Spectrosc. 34 (1999) 71–92.
[6] I.V. Koptyug, K.V. Kovtunov, S.R. Burt, M.S. Anwar, C. Hilty, S.-I. Han, A. Pines, R.Z. Sagdeev, J. Am. Chem. Soc. 129 (2007) 5580–5586.
[7] M. Goldman, H. Jóhannesson, O. Axelsson, M. Karlsson, Magn. Reson. Imag. 23 (2005) 153–157.
[8] F. Reineri, A. Viale, G. Giovenzana, D. Santelia, W. Dastru, R. Gobetto, S. Aime, J. Am. Chem. Soc. 130 (2008) 15047–15053.
[9] L.-S. Bouchard, S.R. Burt, M.S. Anwar, K.V. Kovtunov, I.V. Koptyug, A. Pines, Science 319 (2008) 442–445.
[10] J.F. Dechent, L. Buljubasich, L.M. Schreiber, H.W. Spiess, K. Münnemann, Phys. Chem. Chem. Phys. 14 (2012) 2346.
[11] M. Haake, J. Natterer, J. Bargon, J. Am. Chem. Soc. 118 (1996) 8688–8691.
[12] H. Jóhannesson, O. Axelsson, M. Karlsson, CR Phys. 5 (2004) 315–324.
[13] K.L. Ivanov, A.V. Yurkovskaya, H.-M. Vieth, J. Chem. Phys. 128 (2008). 154701-154701-13.
[14] S.E. Korchak, K.L. Ivanov, A.V. Yurkovskaya, H.-M. Vieth, Phys. Chem. Chem. Phys. 11 (2009) 11146.
[15] L. Buljubasich, M. Franzoni, H. Spiess, K. Münnemann, J. Magn. Reson. 219 (2012) 33–40.
[16] T. Jonischkeit, U. Bommerich, J. Stadler, K. Woelk, H.G. Niessen, J. Bargon, J. Chem. Phys. 124 (2006). 201109-201109-5.
[17] D. Canet, S. Bouguet-Bonnet, C. Aroulanda, F. Reineri, J. Am. Chem. Soc. 129 (2007) 1445–1449.
[18] E. Vinogradov, A.K. Grant, J. Magn. Reson. 194 (2008) 46–57.
[19] M.B. Franzoni, L. Buljubasich, H.W. Spiess, K. Münnemann, J. Am. Chem. Soc. 134 (2012) 10393–10396.
[20] M.B. Franzoni, D. Graafen, L. Buljubasich, L.M. Schreiber, H.W. Spiess, K. Münnemann, Phys. Chem. Chem. Phys. 15 (2013) 17233.
[21] K. Ivanov, A. Pravdivtsev, A. Yurkovskaya, H.-M. Vieth, R. Kaptein, Prog. Nucl. Magn. Reson. Spectrosc. 81 (2014) 1–36.
[22] R.R. Ernst, G. Bodenhausen, A. Wokaun, Principles of Nuclear Magnetic Resonance in One and Two Dimensions, Clarendon Press; Oxford University Press, Oxford [Oxfordshire]; New York, 1987.

[23] M.H. Levitt, Spin Dynamics: Basics of Nuclear Magnetic Resonance, John Wiley & Sons, Chichester, England; Hoboken, NJ, 2008.
[24] J. Colell, P. Türschmann, S. Glöggler, P. Schleker, T. Theis, M. Ledbetter, D. Budker, A. Pines, B. Blümich, S. Appelt, Phys. Rev. Lett. 110 (2013) 137602.
[25] S. Glöggler, B. Blümich, S. Appelt, Top. Curr. Chem. 335 (2013) 1–22.
[26] P. Türschmann, J. Colell, T. Theis, B. Blümich, S. Appelt, Phys. Chem. Chem. Phys. 16 (2014) 15411–15421.
[27] T. Ratajczyk, T. Gutmann, S. Dillenberger, S. Abdulhussaein, J. Frydel, H. Breitzke, U. Bommerich, T. Trantzschel, J. Bernarding, P.C. Magusin, G. Buntkowsky, Solid State Nucl. Magn. Reson. 43–44 (2012) 14–21.
[28] E. Danieli, J. Perlo, B. Blümich, F. Casanova, Ange. Chem. – Int. Ed. 49 (2010) 4133–4135.
[29] E. Danieli, J. Perlo, A.L.L. Duchateau, G.K.M. Verzijl, V.M. Litvinov, B. Blümich, F. Casanova, ChemPhysChem (2014). n/a–n/a.
[30] H. Carr, E. Purcell, Phys. Rev. 94 (1954) 630–638.
[31] S. Meiboom, D. Gill, Rev. Sci. Instrum. 29 (1958) 688–691.
[32] N. Lukzen, K. Ivanov, V. Sadovsky, R. Kaptein, R. Sagdeev, Dokl. Phys. Chem. 449 (2013) 44–47.
[33] L. Buljubasich, I. Prina, M. Franzoni, K. Münnemann, H. Spiess, R. Acosta, J. Magn. Reson. 230 (2013) 155–159.
[34] L. Buljubasich, I. Prina, M. Franzoni, R. Acosta, Micropor. Mesopor. Mater. http://dx.doi.org/10.1016/j.micromeso.2014.08.0391.
[35] I. Prina, L. Buljubasich, R.H. Acosta, J. Phys. Chem. Lett. 4 (2013) 3924–3928.
[36] A. Allerhand, J. Chem. Phys. 44 (1966) 1–9.
[37] R. Freeman, H.D.W. Hill, J. Chem. Phys. 54 (1971) 301–313.
[38] T. Gullion, D.B. Baker, M.S. Conradi, J. Mag. Reson. (1969) 89 (1990) 479–484.
[39] L. Buljubasich, M.B. Franzoni, K. Münnemann, Top. Curr. Chem. 338 (2013) 33–74.